Carbohydrate Polymers 339 (2024) 122243

Contents lists available at ScienceDirect

Carbohydrate Polymers

journal homepage: www.elsevier.com/locate/carbpol

Chemical mapping of xyloglucan distribution and cellulose crystallinity in cotton textiles reveals novel enzymatic targets to improve clothing longevity

Max R. Kelly [a,*,1], Neil J. Lant [b], Rolando Berlinguer-Palmini [c], J. Grant Burgess [a]

[a] School of Natural and Environmental Sciences, Ridley Building, Newcastle University, Newcastle upon Tyne NE1 7RU, United Kingdom
[b] Procter and Gamble, Newcastle Innovation Centre, Whitley Road, Longbenton, Newcastle upon Tyne NE12 9TS, United Kingdom
[c] Bioimaging unit, William Leech Building, Medical School, Newcastle University, Newcastle upon Tyne NE1 7RU, United Kingdom

ARTICLE INFO

Keywords:
Cellulose Characterisation
Crystallinity
Xyloglucan
Bioimaging
Enzymes

ABSTRACT

Pilling is a form of textile mechanical damage, forming fibrous bobbles on the surface of garments, resulting in premature disposal of clothing by consumers. However, our understanding on how the structural properties of the cellulosic matrix compliment the three-dimensional shape of cotton pills remains limited. This knowledge gap has hindered the development of effective 'pillase' technologies over the past 20 years due to challenges in balancing depilling efficacy with fabric integrity preservation. Therefore, the main focus here was characterising the role of cellulose and the hemicellulose components in cotton textiles to elucidate subtle differences between the chemistry of pills and fibre regions involved in structural integrity. State-of-the-art bioimaging using carbohydrate binding modules, monoclonal antibodies, and Leica SP8 and a Nikon A1R confocal microscopes, revealed the biophysical structure of cotton pills for the first time. Identifying regions of increased crystalline cellulose in the base of anchor fibres and weaker amorphous cellulose at dislocations in their centres, enhancing our understanding of current enzyme specificity. Surprisingly, pills contained a 7-fold increase in the concentration of xyloglucan compared to the main textile. Therefore, xyloglucan offers a previously undescribed target for overcoming this benefit-to-risk paradigm, suggesting a role for xyloglucanase enzymes in future pillase systems.

1. Introduction

The formation of entangled fibres that create bobble-like structures known as pills on clothing are one of the most visible signs of garment ageing, resulting in consumer dissatisfaction and ultimately clothing discard (Choudhury, 2017; Cooper et al., 2013). Thus, the premature disposal of pilled textiles has created a significant environmental burden, whilst the production of new clothing continues to increase in the era of 'fast fashion', requiring more natural resources and materials (EMF, 2017). The formation of pilling (comprised of the pill head and anchor fibres secured to the main textile 'bulk' fibres) is well described within the literature, categorised by distinctive stages of development which include fuzz formation, entanglement, growth and removal (Cooke, 1983; Gintis & Mead, 1959) as highlighted in Fig. 1.

To reduce pilling, initial and more aggressive physical and chemical solutions such as singeing, alkaline treatments, and surface resins, including formaldehyde-based resins (Tomasino, 1992) and sodium hydroxide (NaOH) treatments have been employed (Stryckman & Leclereq, 1972). However, this also introduces undesirable characteristics, such as reduced fibre softness (Bui et al., 2008; Choudhury, 2017), which often requires a fabric softener to counteract (Montazer & Sadighi, 2006). Enzymatic alternatives such as cellulases that are incorporated within detergent formulations offer a more environmentally conscious approach to these often-toxic chemical counterparts (Niyonzima, 2019).

One of the first enzyme technologies, developed in the 1980s, that provided a pilling benefit to detergents was Celluzyme®, a mixture of several cellulases including *endo*-β-1,4-glucanases, cellobiohydrolases,

* Corresponding author.
E-mail addresses: max.kelly@plymouth.ac.uk (M.R. Kelly), lant.n@pg.com (N.J. Lant), rolando.berlinguer-palmini@ncl.ac.uk (R. Berlinguer-Palmini), grant.burgess@newcastle.ac.uk (J.G. Burgess).
[1] Present address: School of Biological and Marine Sciences, University of Plymouth, Plymouth, PL4 8AA, United Kingdom

https://doi.org/10.1016/j.carbpol.2024.122243
Received 15 March 2024; Received in revised form 2 May 2024; Accepted 7 May 2024
Available online 8 May 2024

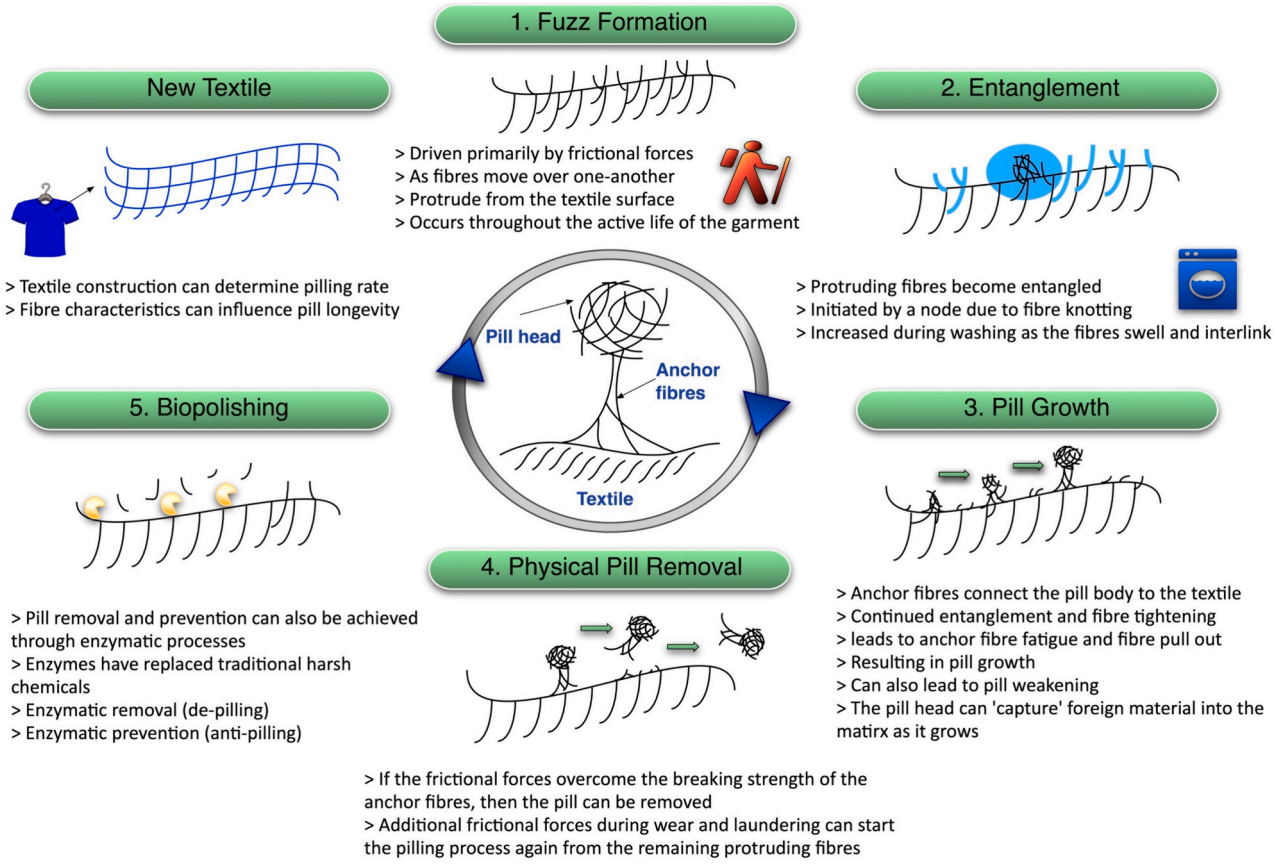

Fig. 1. The stages of pill development and removal.

and β-Glucosidases originating from the fungus, *Humicola insolens* and supplied by Novozymes, then Novo Nordisk (Schou et al., 1993). However, under collaboration between Procter and Gamble (P&G) and Novozymes, it was realised that isolation of a single endo-β-1,4-glucanase with a glycoside hydrolase (GH) family 45 (GH45) catalytic domain linked to a family 1A carbohydrate binding module (CBM), could improve a so-called benefit-to-risk paradigm; whereby the pilling benefit (removal/de-pilling or prevention/anti-pilling) was maintained but the tensile strength loss (risk) was reduced compared to Celluzyme®. This was due to the absence of the full cellulose degradation arsenal in Celluzyme®, where cellobiohydrolases and β-Glucosidases aid in the conversion of cellulose to glucose (Maurer, 1997). This enzyme was commercially named Carezyme® (Caparrós et al., 2012) and the catalytic core structure is described in Davies et al. (1996). Carezyme® Premium was later developed from the *Thielavia terrestris* endoglucanase (GH45), where the protein engineered variant provided better stability in liquids compared to the parent molecule. Carezyme® Premium provided a superior pilling benefit and stability compared to Carezyme® (Schülein, 2000).

Endo-beta-1,4-glucanases, primarily GH45 archetypes including those derived from *H. insolens*, have dominated the global market for laundry application (Caparrós et al., 2012; Koga et al., 2008). The presence of family 1A CBMs within these enzyme structures enable pilling benefits as they facilitate binding to crystalline cellulase. CBMs are non-catalytic proteins that enhance enzyme activity through specific binding with target carbohydrates (Boraston et al., 2004). Crystalline cellulose contains highly ordered cellulose chains and a higher degree of hydrogen bonding compared to amorphous cellulose (Martínez-Sanz et al., 2017). Consequently, crystalline cellulose provides greater structural integrity with higher tensile strength and is less susceptible to enzyme degradation compared to the amorphous counterpart (Hao et al., 2016; Pethrick, 2005). Enzymes targeting crystalline cellulose are often described as 'care' cellulases by detergent manufacturers since they contribute to the physio-chemical properties of the fabric including pilling benefits, improved softness, and colour fidelity (Al-Ghanayem & Joseph, 2020; Arja, 2007). Whereas, cellulases that target amorphous cellulose provide benefits including anti-redeposition, colour care, and whiteness are often described as 'cleaning' cellulases. Whilst care cellulases are active on both crystalline and amorphous cellulose, cleaning cellulases are active towards amorphous cellulose only.

Since the late 1990s and Carezyme® Premium, there has been a lack of novel pilling technologies able to further improved this benefit-to-risk ratio. Detergent manufacturers have tried to mitigate pilling effects, for example, through cellulase-CBM hybrid constructs, engineering variants of particular GH families (often GH5, GH7, and GH45), and modifying the enzyme-CBM linker length (Alapuranen et al., 2007; Juntunen et al., 2018; Juntunen et al., 2020). However, understanding details in the performance of different commercial cellulases is often reliant on the patent literature, as there are limited studies comparing their benefits and no study comparing the pilling efficacy.

The absence of specific de-pilling or anti-pilling enzymes, or collectively, 'pillases', in more recent years, that can break the benefit-to-risk paradigm may be explained by the lack of characterisation in the biophysical structure of a pill to help direct the specificity of commercial enzymes. Here, the biophysical structure describes the localised distribution of amorphous and crystalline cellulose, surface characteristics of the individual fibres during pilling, and the structural role of hemicelluloses in pilling.

Furthermore, by understanding whether the biophysical structure of a pill is compositionally different to the main textile fibres, new insights could be gained that will lead to an improved benefit-to-risk ratio by targeting substrates that are present at higher concentrations in the pill compared to the main textile. Morgado et al. (2000) physically removed pills from lyocell fabric with a razor blade to compare the crystallinity

Table 1
Textile characteristics used for bioimaging analysis (Fruit of the Loom®) and testing the de-pilling performance of different commercial enzymes (Swissatest® (252)).

Garment	Colour	Fibre composition	Construction	Weight (g/m^2)	Crystallinity (XRD)	Used for
Fruit of the Loom® Original T-shirt (61082)	White	100 % cotton	Fine knit gauge	135	79.5 %	Understand the biophysical structure of pilling
Swissatest® pilling monitor 252	Black, blue, red, green stripes	94 % cotton, 6 % elastane	Printed jersey	240	78.7 %	Measure de-pilling performance of commercial cellulases

index (CI) (ratio of crystalline to amorphous cellulose) with the remaining textile. The study found no differences in the CI between the pill and textile. However, the study did not differentiate how the crystallinity is distributed within the pills and how this may differ when compared to the main textile.

In addition to cellulose, cotton also contains hemicellulose components, such as xylan, xyloglucan, and mannan, which facilitate cross-linking of cellulose in plant cell-walls, enabling a compact matrix within pectic polysaccharides (Ansell & Mwaikambo, 2009). While much of the non-cellulosic polysaccharide content is removed during the textile manufacturing process, some materials remain (Runavot et al., 2014) and the potential role of these components in pilling has not yet been studied. Furthermore, the majority of the mechanistic understanding of pilling was developed in the second half of the 20th century (Baird et al., 1956; Ukponmwan et al., 1998). Therefore, new biotechnological approaches are also needed to elucidate potentially uncharacterised enzymatic targets for future pillases. For example, fluorescent proteins ('probes') conjugated to CBMs have been used to identify structural differences in cellulosic fibres (Gourlay et al., 2015; Novy et al., 2019). However, identification of spatial differences in the amorphous and crystalline cellulose content of pilled cotton textiles remains unexplored.

We hypothesised there would be distinct spatial differences in the distribution of cellulose crystallinity and hemicellulose composition between cotton pills and bulk fibres. These subtle differences in the cellulosic matrix of cotton could subsequently be targeted through the specificity of enzymes to preferentially remove cotton pills. To test this hypothesis, scanning electron microscopy (SEM) and state-of-the-art bioimaging protocols were developed with the use of CBMs and monoclonal antibodies (mAbs) conjugated to fluorescent proteins to a) characterise the distribution of crystalline and amorphous cellulose in pilled textiles; b) characterise the distribution of hemicellulose in pilled textiles; c) use these findings to identify differences in the cellulosic matrix between pills and the main textile fibres that could then be enzymatically targeted to overcome the benefit-to risk-paradigm; and d) compare the de-pilling performance of current commercial care and cleaning cellulases to highlight how the cellulosic structure of pills relates to enzyme architecture and performance.

2. Material and methods

2.1. Measuring textile crystallinity

To measure the CI of the textiles studied (Table 1), X-ray diffraction (XRD) was conducted using an XRD2 (PANalytical X'Pert). A square piece of each fabric was clipped into a zero-background holder. A preliminary scan between 5 and 120° 2theta was completed to determine peak location before higher resolution scans were completed in the 2theta range: 10–70°, step size = 0.033°, time per step = 2 s, divergence slit = 1°, beam mask = 20 mm, receiving slit = 0.5° at wavelength Cu K, 1.5406 Å. The CI of each fabric was calculated according to the empirical method derived by Segal et al. (1959):

$$\mathrm{CI}(\%) = \frac{\mathrm{I}_{002} - \mathrm{I}_{\mathrm{am}}}{\mathrm{I}_{002}} \times 100$$

Where I_{002} is the maximum intensity of diffraction of the 002 lattice peak at a 2θ angle (between 21 and 23°), which represents both crystalline and amorphous cellulose. I_{am} is the amorphous diffraction intensity taken where the intensity is at minimum between 18 and 20° (often reported at $2\theta = 18°$) (Ghaffar, 2017; Hewetson et al., 2016).

Table 2
Fluorescently labelled carbohydrate binding modules and monoclonal antibodies used to characterise the biophysical structure of pilled textiles.

Probe	Fluorescence	Ligand specificity	Reference
CBM44	mCherry	Amorphous cellulose	(Gourlay et al., 2015)
CBM2a	GFP	Crystalline cellulose	(Gourlay et al., 2015)
CBM27a	GFP	β-1,4-mannooligosaccharides	(Boraston et al., 2003)
CBM3a	GFP	Crystalline cellulose	(Jauris et al., 1990)
CBM22a	GFP	Xylans	(Moraïs et al., 2016)
CBM10a	GFP	Crystalline cellulose	(Raghothama et al., 2000)
CBM2b-2	GFP	1,4-β-xylans	(Simpson et al., 2000)
CBM6a	GFP	1,3-β-glucans	(van Bueren et al., 2005)
LM15	GFP	Xyloglucan, XXXG motif	(Marcus et al., 2008)
LM21	GFP	Galacto(*gluco*)mannan	(Marcus et al., 2010)
LM22	GFP	(1 → 4)-β-d -(gluco)mannan	(Marcus et al., 2010)
LM24	GFP	Xyloglucan (XG), XLLG motif	(Pedersen et al., 2012)
LM25	GFP	Xyloglucan (XG), XLLG, XXLG and XXXG motifs	(Pedersen et al., 2012)

2.2. Pre-pilling textiles for pill removal and imaging

White Fruit of the Loom® Original T-shirts (product code 61082), supplied by BTC Activewear, Wednesbury, UK, were pre-pilled for 20 cycles (cotton short wash: 40 °C, 85 min, 1600 RPM spin) in an Electrolux Wascator FOM71CLS automated washing machine. New T-shirts without any pre-pilling were also used as a control. A 1 × 1 cm swatch was removed from the fabric (by scissor cutting) containing a visible pill attached in the centre of the swatch. The swatch was then folded in half and kept in place with a small drop of epoxy resin with the pill at the edge of the fold for ease of imaging.

2.3. Scanning electron microscopy (SEM) to characterise the physical structure of pills

A Tescan Vega scanning electron microscope was used to image and characterise the physical structure of pilled and new (untreated) cotton textiles. The samples were prepared using a Baltec Critical Point Dryer (Electron Microscopy Research Services, Newcastle University, UK). Each cotton swatch was mounted on aluminium stubs with Achesons Silver ElectroDag or carbon discs, before 15 mm gold coating using a Polaron SEM coating unit.

2.4. Bioimaging: fluorescent labelling of whole pills protocol

Pills were incubated with different CBMs and mAbs conjugated to fluorescent proteins to image and characterise the cellulosic components of pilling phenomena and determine the most suitable CBMs/mAbs for subsequent image analysis (heading 2.5) (Table 2). mAbs are laboratory-produced molecules engineered to recognise and bind to specific epitopes (Singh et al., 2018). Fluorescent labelling was run in triplicate for each CBM or mAb with methods adapted from Willats et al. (2001) where a single pilled swatch was incubated in 5 % (w/v) milk powder in PBST (1X phosphate buffered saline and 0.1 % TWEEN®) for 1 h to prevent non-specific binding. CBMs were then added (10 μg/mL) and left to incubate for 90 min at 50 RPM in 24 well plates covered by aluminium foil to prevent bleaching. After incubation, each pill was washed immediately in PBS (1x phosphate-buffered saline) and again four more times in clean PBS for 5 min during each wash step to remove the excess CBM. Control pills were prepared in the same protocol without the addition of a CBM. However, mAbs were added in a 10-fold dilution within fresh PBST and left to incubate for 2 h. Pills were then washed three times with clean PBS to remove excess primary antibody. Secondary antibody of IgG conjugated to fluorescein isothiocyanate (FITC), either anti-rat or anti-mouse as appropriate for the selected mAbs, was then diluted 100-fold in PBST and incubated in the dark for 2 h. Two further controls were also prepared by removing either the primary antibody or both primary and secondary antibodies. Pills were then washed four times in fresh PBS.

The images were acquired using a Nikon A1R confocal microscope and a Leica SP8 microscope with *Z*-stacking. A Leica SP8 confocal microscope able to detect any wavelength between 400 and 800 nm and excite any wavelength between 470 and 670 nm (using a white laser) was initially used to assess autofluorescence from the controls and probed samples to ensure the optimal acquisition settings for imaging pilled textiles (to remove background autofluorescence that may interfere with imaging). Videos were also created using Nikon NIS-Element (when acquired with the Nikon A1R) or the Leica LasX software (when acquired with Leica SP8) to visualise the complete structure of pills (links to which are highlighted in the figures).

2.5. Bioimaging: characterising the biophysical structure of pills

To help identify where commercial enzyme constructs bind to and subsequently degrade different regions of pills, the crystallinity distribution of pills was characterised. CBM44-mCherry (targeting amorphous cellulose) and CBM2a-GFP (targeting crystalline cellulose) were initially selected based on the methods of Gourlay et al. (2015) and were purchased from NZYtech (https://www.nzytech.com). These CBMs were also compared to the binding affinity of CBM3a, 6a and 10a, kindly donated by Professor William Willats (Newcastle University) to ensure the optimal CBMs for imaging textile crystallinity were used (Table 2). Comparison of pill crystallinity was identified using two different wavelengths of light to acquire images: GFP is excited at 499 nm and is detected between 506 and 560 nm highlighting crystalline cellulose through binding with CBM2a-GFP, whereas mCherry is excited at 586 nm and is detected between 594 and 795 nm, highlighting amorphous cellulose through binding with CBM44-mCherry. For visual comparison between CBM and mAb binding regions with the overall structure of pilled textiles, the autofluorescence signal due to the presence of an optical brightener (commonly used in textile manufacturing of white cotton fabrics to improve colour appearance) was also imaged. This autofluorescence signal was excited at 405 nm and collected between 410 nm and 470 nm. The remaining CBMs and mAbs (Table 2) were used to identify differences in the hemicellulose components of pilling compared to main textile fibres that may provide novel enzymatic targets to overcome the benefit-to-risk paradigm.

Table 3
Commercial care (crystalline targeting) and cleaning (amorphous targeting) cellulases tested to compare the de-pilling performance towards Swissatest® (252) fabric.

Enzyme	Type	Supplier	Source	Structure
Carezyme® 4500L	Care	Novozymes	*Humicola insolens*	GH45 + CBM1
Carezyme® Premium 4500L Formerly marketed as Renozyme®	Care	Novozymes	*Thielavia terrestris*	GH45 + CBM1
Revitalenz® 200	Care	Genencor (now IFF)	*Staphylotrichum coccosporum*	GH45 + CBM 1
Biotouch® FCL 75	Care	AB Enzymes	*Melanocarpus albomyces* (catalytic domain)	GH45 + CBM1
Whitezyme® 2.0L	Cleaning	Novozymes	*Paenibacillus polymyxa*	GH44
Celluclean® 5T	Cleaning	Novozymes	*Bacillus sp.* AA349	GH5 + CBM 17 + 28
Celluclean® 5000L Formerly marketed as Endolase®	Cleaning	Novozymes	*Humicola insolens*	GH7
Biotouch® FLX1	Cleaning	AB Enzymes	*Melanocarpus albomyces*	GH45

2.6. Bioimaging: cross sectioning fibres

For a deeper understanding of crystalline and amorphous cellulose distribution in pilled textiles, differences in the crystallinity between the outer perimeter (often described as the 'skin' or 'shell' of a fibre (Martínez-Sanz et al., 2017; Rous et al., 2006)) and fibre core were imaged and characterised. Textiles were embedded in the middle of a double layer of epoxy resin to maintain the structure of the fabric before a microtome was used to cut 150 μm sections of the embedded fabric at a frequency of 12 Hz and an amplitude of 0.5 mm. The sections were then probed in the same manner as heading 2.4. The cross sectioned fabric was transferred to a microscope slide with a drop of Citifluor anti-fading agent, covered with a cover slip and sealed with transparent nail varnish, then left to dry in the dark to prevent bleaching.

2.7. Bioimaging: image processing and analysis

All images were processed using SVI's Huygens Professional V19.04 imaging software (SVI, Hilversum, Netherlands). To accurately quantify and compare fluorescence intensity as a measure of CBM and mAb binding affinity (proportional to the concentration of the probed cellulosic components), images were deconvolved prior to analysis (Biggs, 2010). To do this, the acquisition settings were kept constant for intensity, gain, magnification, and thickness (number of steps and width) of the *Z*-stack. The Nyquist sampling parameters (Landau, 1967) were also predetermined using the SVI microscopy Nyquist calculator (https://svi.nl/NyquistCalculator). This allows for optimal voxel size when capturing imaging to permit post deconvolution and improve the image resolution, particularly in the Z-plane. Huygens 'Object Analyser' function was used to remove background 'noise' of the images if required before calculating the average intensity of the fluorophores in each image (https://svi.nl/Huygens-Object-Analyzer). The threshold and seed parameters were also kept constant when comparing intensities between labelled pills (Fig. S1). Colocalization analysis was carried out my measuring the co-occurrence and correlation of CBM44 and CBM2a binding with Huygens 'Colocalization Analyser' function. Co-occurrence describes the extent of spatial overlap between two fluorophores. Co-occurrence measurements using Manders' M1 and M2 coefficients are often best utilized to determine what proportion of a molecule is present

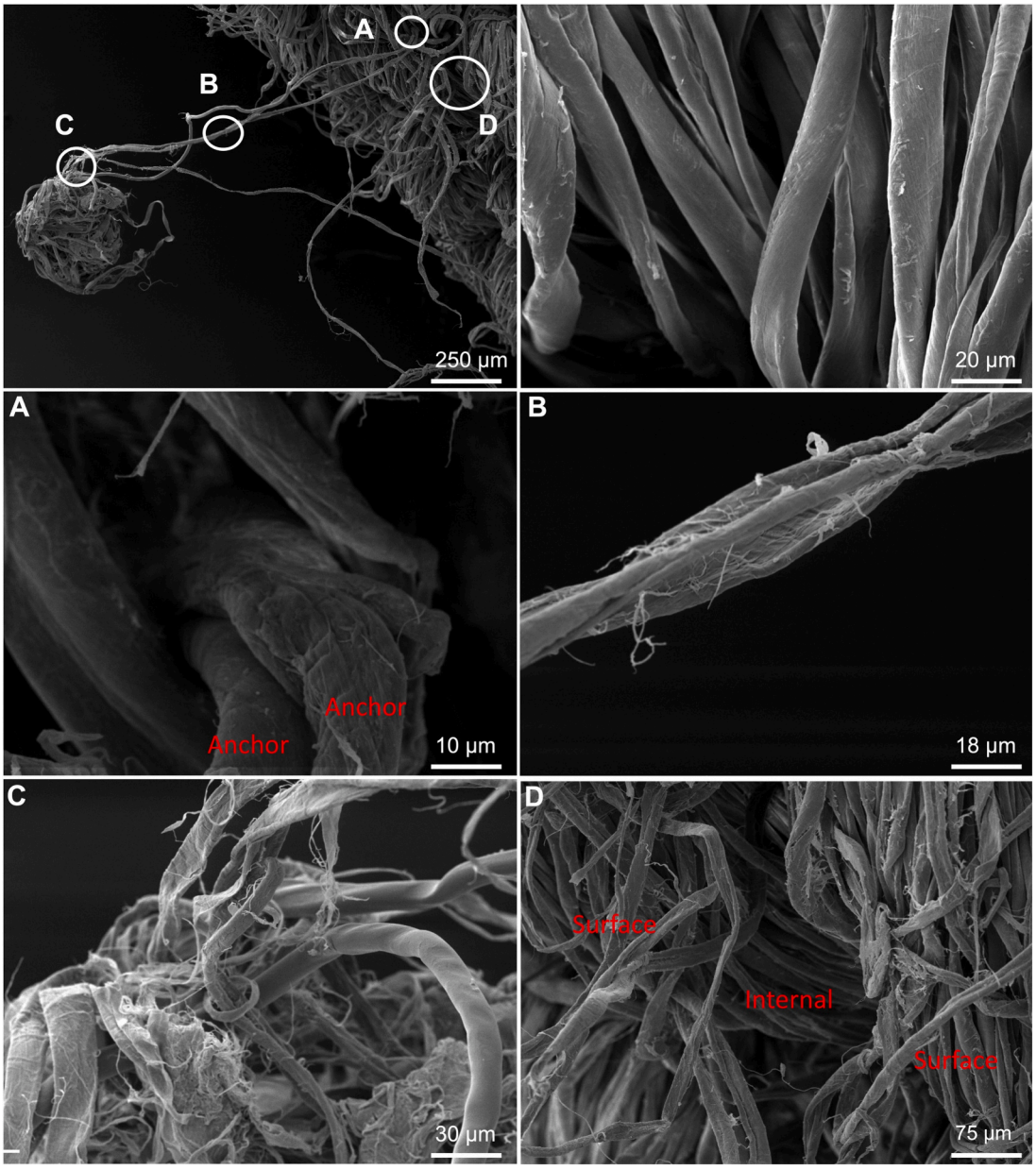

Fig. 2. Different regions of a cotton textile pill after 20 cycles of repeated washing. Whole pill (top left) compared to new (untreated) textile fibres (top right). Images highlight the base of the anchor fibre (A), central region of the anchor fibre (B), anchor fibre and pill head attachment (C) and the surface and internal fibres near the base of the pill (D). Images were acquired using a Tescan Vega scanning electron microscope.

within a particular area (Aaron et al., 2018). Correlation determines the degree to which the abundance of two spatially overlapping fluorophores are related to each other (degree of correlative variation between two channels) measured using Pearson's or Spearman's coefficient (Krichevsky & Bonnet, 2002).

2.8. Comparing the de-pilling performance of commercial enzymes

A total of 108 Swissatest® article 252 (Swissatest® (252)) fabrics were pre-pilled using a 20 cycle washing programme as Swissatest® (252) fabrics are commonly used by detergent manufacturers to measure enzyme performance towards pilling. Four cleaning and four care commercial enzymes (Table 3) were added to separate washing machines (Miele, Honeycomb care: W3622) at a concentration of 1 ppm (parts per million) with 35 mL (37.8 g) of Ariel® liquid detergent (UK) containing twelve Swissatest® (252) fabrics. A control of only Ariel® detergent was also used for comparison towards enzyme performance. The fabrics were washed by a cotton short programme (40 °C, 1600 RPM spin, 85 min) for 5 cycles. To avoid bias from any slight differences in performance between appliances, treatments were rotated after each cycle between the different washing machines within the set.

2.8.1. Measuring the de-pilling performance of commercial enzymes

After washing, the Swissatest® (252) fabrics were imaged and analysed using DigiEye machinery and software (Luo et al., 2001) (VeriVide Ltd., Leicester, U.K.) to calculate the colour difference (ΔE) described in Tkalcic and Tasic (2003) compared to a new (un-treated) reference Swissatest® (252) fabric as a measure of pilling. Within DigiEye, images were taken using a fixed DSLR camera (shutter speed of 1/2.5 of a second and an aperture width of 7.1 mm) in a controlled D65 illumination cabinet. Images are viewed on a calibrated liquid-crystal display monitor using the Engauge Digitizer chart v 3.5. The camera is also

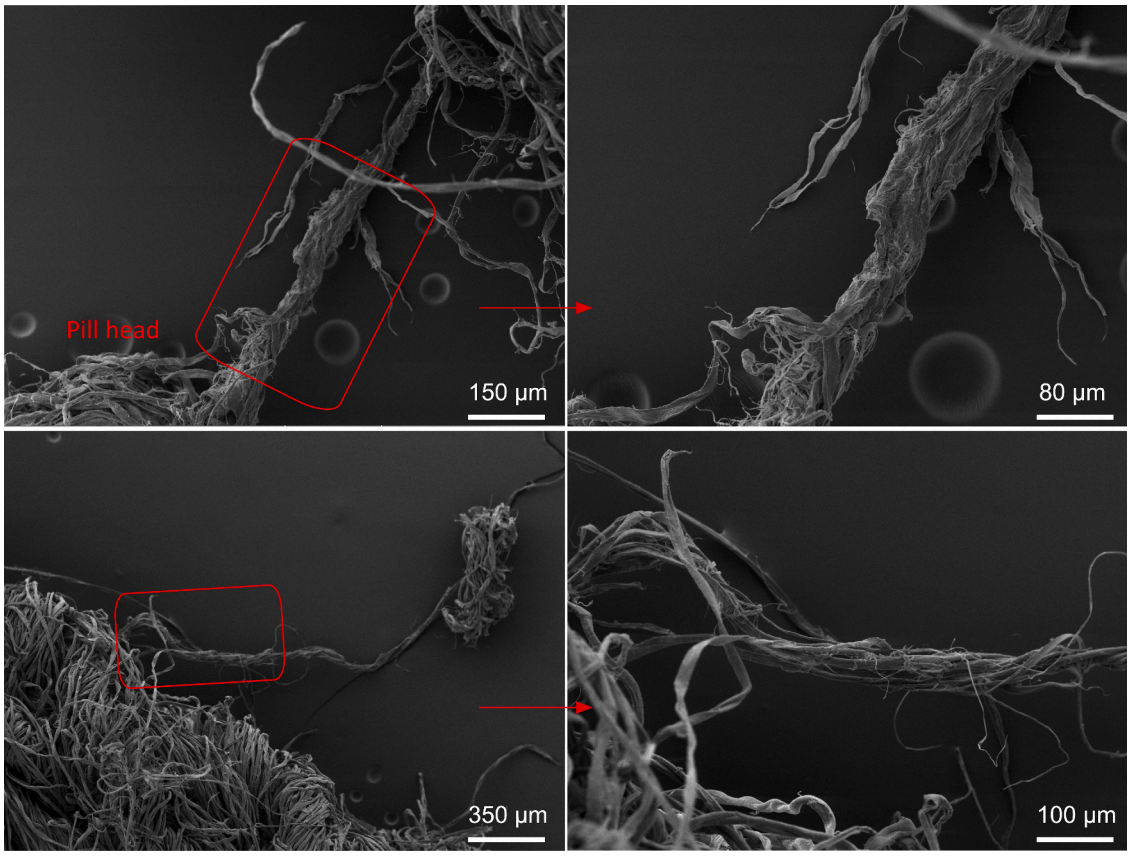

Fig. 3. Combined pill anchor fibres. Multiple, twisted anchor fibres that form a thicker, single large strand connecting the pill head to the textile represents a previously undescribed stage in pill formation. Images of the two different pills were acquired using a Tescan Vega scanning electron microscope.

calibrated using the Digitizer chart which characterises the RGB signal response to the CIE (International Commission on Illumination) specification with fixed lighting conditions in the illumination cabinet (Robertson, 1977). Colour measurements of L* (lightness), a* (green-red), and b* (blue-yellow) were recorded for each coloured strip (blue, black, red and green) of each Swissatest® (252) swatch and compared to an untreated new reference (Fig. S3). L*, a*, b* values are obtained through the DigiEye software by calculating the RGB values of every pixel across the fabric to calculate an overall mean. The RGB values are then converted to XYZ D65/10 (measured XYZ values for D65 illuminant a 10° observer) (Derhak, 2015), which is the amount of red, green, and blue response of the light-sensitive cone cells of the eye needed to match the colour in the specified illuminant. White fibres protrude through the coloured dye during pre-pilling (heading 2.8) and form visible fuzz and pills on the surface of the fabric that can be distinguished between the coloured backgrounds of the dye. This allowed the overall ΔE to be calculated for each commercial enzyme and can be used as a proxy for measuring de-pilling. The lower the ΔE value, the greater the pill removal (removal of white protruding pills) as the fabric colour is closer to a new fabric reference.

2.9. Statistical analyses

The colour difference (ΔE) values across Swissatest® (252) fabrics for each enzyme were conformed to homogeneity of variances using Levene's test (Rstudio, version 4.1.1), before conducting a one-way analysis of the variance (ANOVA) to examine the de-pilling performance of different care and cleaning cellulases. *Post hoc* TukeyHSD (Tukey's honest significance test) was used to determine significant differences between pairwise comparisons.

3. Results

3.1. Physical structure of pills

SEM was used as an initial tool to elucidate the physical structure of different regions within pills (Fig. 2) and to compare these potential differences with subsequent bioimaging analysis. Qualitatively, after 20 cycles of repeated washing, individual fibres were considerably frayed compared to new, smooth fibres without any washing (Fig. 2). Exposed surface fibres also showed a substantially higher degree of fraying compared to internal main textile fibres (Fig. 2D). The base of the anchor fibres (Fig. 2A) showed signs of potential tensile stress with tearing across the vertical axis of the fibres but a lower degree of fraying compared to the mid-section of an anchor fibre (Fig. 2B) and the pill head (Fig. 1C). In addition, the central region of anchor fibres were often compressed and twisted (Fig. 1B), whereas the pill head contains a variety of entangled frayed fibres with different morphologies, including foreign material mixed within. Interestingly, multiple anchor fibres can become twisted, forming a single large strand connecting the pill head to the textile (Fig. 3), which is previously undescribed in the literature and may be an additional fifth step in the life cycle of a pill (before biopolishing; Fig. 1). Therefore, pills that are formed in this way may require significant enzymatic removal compared to single anchor fibre-forming pills.

3.2. Comparing the skin-core relationship of crystalline to amorphous cellulose within pills and main textile fibres

From the different CBMs tested (CBM families 2a, 3a, 6a, 10a and 44; Table 2), CBM2a and CBM44 were selected as the optimal candidates to identify the crystalline distribution within pilled textiles. This was based

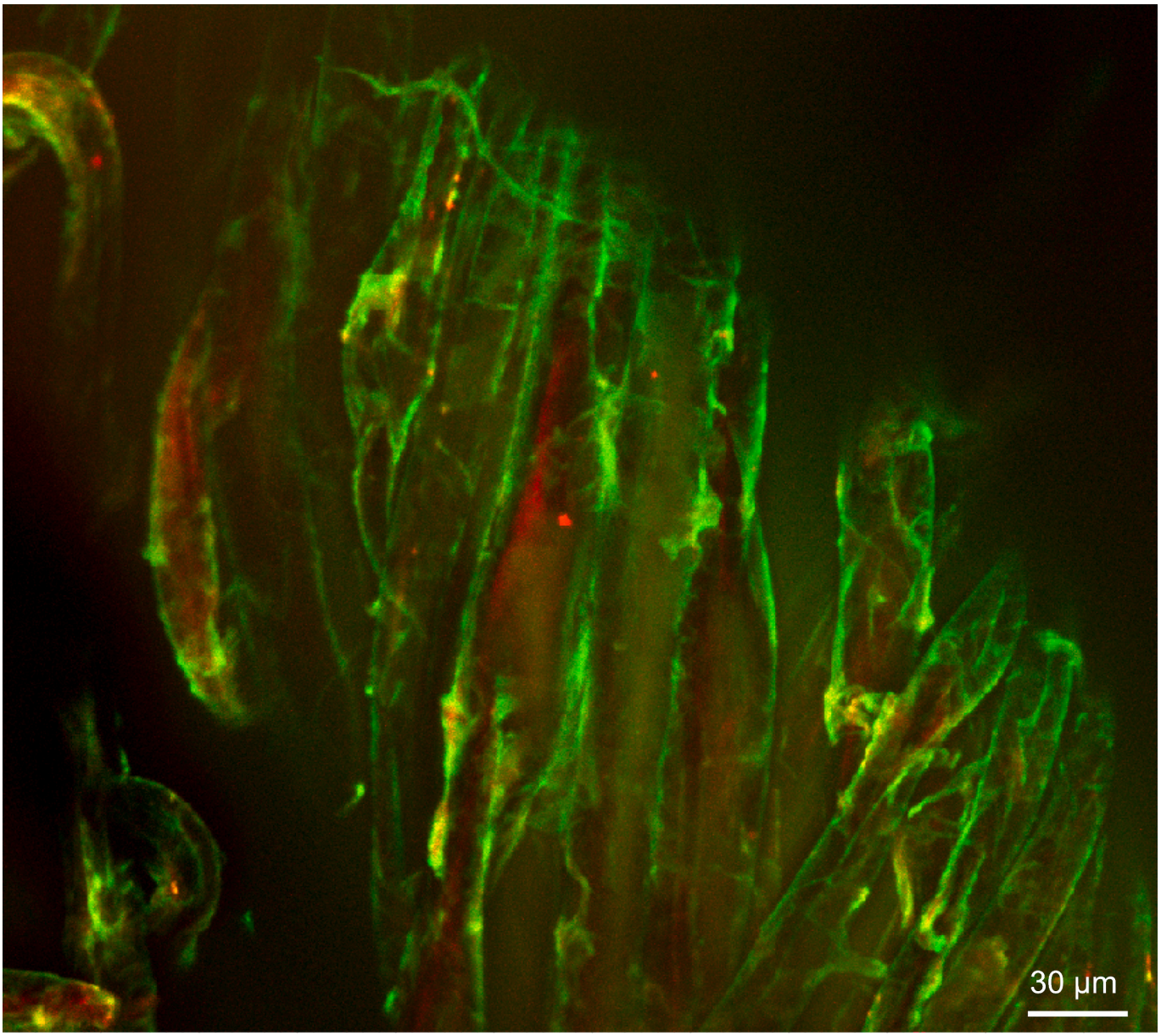

Fig. 4. The distribution of crystalline (green, using CBM2a-GFP) and amorphous cellulose (red, using CBM44-mCherry) within main textile fibres. The image highlights a dominant crystalline skin interspersed by amorphous cellulose. Image acquired by a Nikon A1R confocal microscope and deconvolved using Huygens Professional imaging software.

on binding affinity measured by average fluorophore intensity using Huygens software (Fig. S1). Imaging revealed the skin of cotton main textile fibres (Fig. 4) and pilled fibres (Fig. 5) consisted of predominantly crystalline cellulose, which was interspersed with amorphous cellulose along the fibre. The crystallinity of the cotton T-shirts used for pill characterisation was 79.5 % (Fig. S2), indicating a higher proportion of crystalline cellulose. Co-occurrence measurements using Mander's co-efficient also revealed 79.5 ± 8.1 % of the GFP signal (CBM2a, crystalline cellulose) 'overlaps' with that of the mCherry signal (CBM44, amorphous cellulose) across pilled fibres. Fig. 4 and Fig. 5 suggest the 20 % region of no overlap between the amorphous and crystalline regions may be explained as crystalline cellulose appears in greater concentration along the outer perimeter of the fibre. Mander's analysis also revealed 97 ± 9.2 % of the amorphous cellulose overlaps with crystalline cellulose indicating that amorphous cellulose is more frequently surrounded by crystalline cellulose. To understand the skin-core relationship of crystalline and amorphous cellulose in more detail, the fibres were cross sectioned and imaged. Cross section imaging also revealed a predominant crystalline skin and a crystalline core in main textile fibres (Fig. 6) and anchor fibres (Fig. 7), although the distribution of crystalline and amorphous cellulose was not uniform across all fibres.

3.3. Spatial distribution of crystalline and amorphous cellulose throughout cotton pills

The crystallinity distribution within the different regions of pills (base, anchor, and head) was investigated in greater detail to understand whether there are localised differences between crystalline and amorphous cellulose between these regions and to highlight where cleaning and care cellulases may preferentially target pilling. Concentrated regions of amorphous cellulose were identified in the centre of anchor fibres (Fig. 5 and Fig. 8), particularly, when the fibre was twisted, and within the pill head, whereas the base of the anchor fibre comprised of predominately crystalline cellulose (Fig. 8). On closer inspection, a

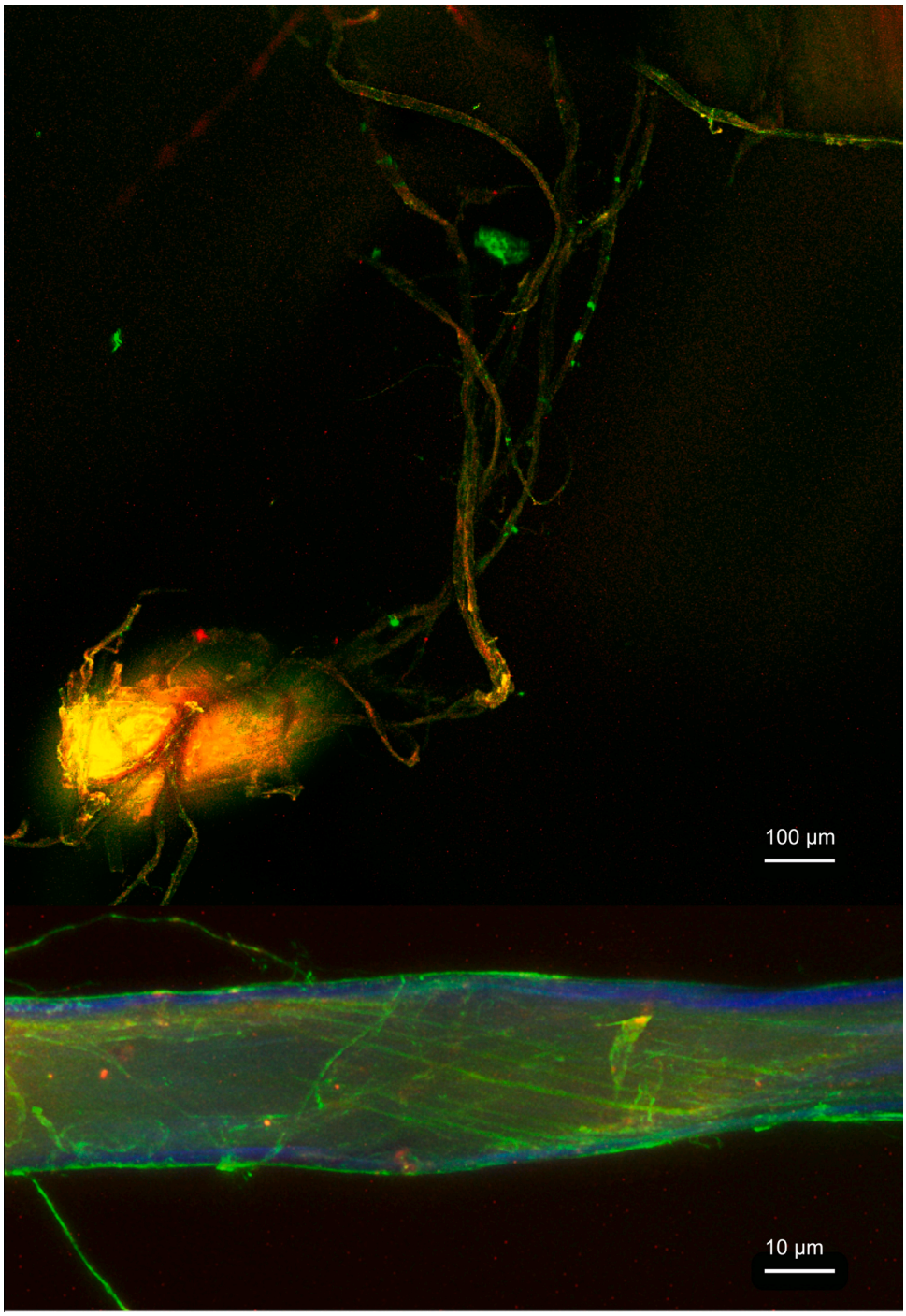

Fig. 5. Crystallinity of pills. The distribution of crystalline (green, using CBM2a-GFP) and amorphous (red, using CBM44-mCherry) cellulose within a pill (top) and pill anchor fibre (bottom). The outline of the anchor fibre is also highlighted in blue due to autofluorescence. 3D MP4 video available (https://figshare.com/s/20f3bb63c0518e5ab431) to show the complete structure of the pill and anchor fibre (https://figshare.com/s/b9dcd6455c1530e8da1c). Images acquired with Nikon A1R confocal microscope.

three-dimensional (3D) render of the anchor fibre at a high magnification (40×) revealed clear differences in these localised areas of increased amorphous cellulose (Fig. 9 and an additional example in Fig. S4). A 3D render visualises isosurfaces of 3D volumes, which provides a surface representation of points with equal intensities in a 3D stack that is the equivalent of a contour line (Hansen & Johnson, 2011). Depth profile mapping confirmed this observation where regions of the fibres completely lacked crystalline cellulose and only amorphous cellulose was found (Fig. 9). Therefore, whilst the entire cotton textile is comprised of 79.5 % crystalline cellulose (Fig. S2), the localised distribution of crystalline and amorphous cellulose can vary throughout the different regions of a pill.

3.4. *Xyloglucan: a novel target for pillase discovery?*

LM25 (xyloglucan targeting) mAb revealed 6.5x ± 3.6 (n = 5) greater fluorophore intensity in pills compared to the main textile fibres of the same pilled fabric. This suggests that whole pills contain on average 6.5x the concentration of xyloglucan compared to the main textile fibres (Fig. 10). Therefore, xyloglucan offers a previously

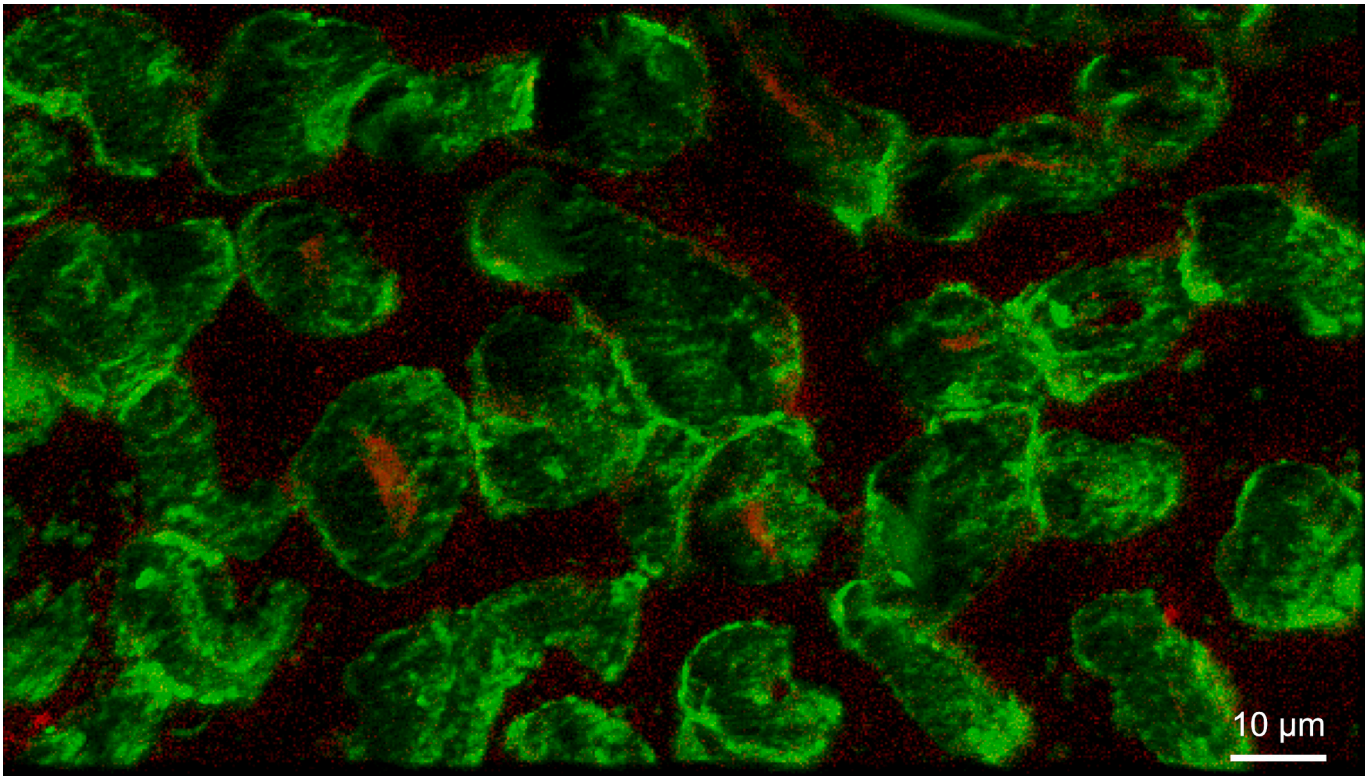

Fig. 6. Crystallinity of bulk textile fibres. Cross section distribution of crystalline (green, using CBM2a-GFP) and amorphous (red, using CBM44-mCherry) cellulose within cotton main textile fibres. Imaged acquired with 40× lens and Nikon A1R confocal microscope.

undescribed target for overcoming the benefit-to-risk paradigm, highlighting the potential of xyloglucanases as an interesting enzyme class to explore for discovery of potentially novel pillases. LM25 provided the greatest binding profile and can be used as a model mAb for identifying regions of xyloglucan in cotton-based textiles. Whereas the binding profiles as measured by fluorophore intensity for LM15, LM24, CBM22a and CBM2b-2 also targeting xyloglucan, were much weaker. Similarly, LM21, LM22 and CBM27a (mannan targeting) had a very weak signal indicating only a very small and potentially insignificant hemicellulose component to target when attempting to provide pilling benefits through enzyme processes.

3.5. *Pilling performance of detergent cellulases*

After 5 cycles of washing, all care cellulases provided a greater de-pilling benefit than all cleaning cellulases (ANOVA, $F(8, 27) = 228.1$, $P < 0.0001$). However, Whitezyme® and Biotouch® FXL1 also provided a significantly greater de-pilling benefit compared to the control of Ariel® detergent only, indicating amorphous targeting cellulases can also provide some pilling benefits during laundry.

4. Discussion

4.1. *The biophysical structure of pills and the resulting implications for commercial cellulases to target pilling*

Cotton textile fibres contained a predominantly crystalline skin and core (Fig. 4 and Fig. 5). However, we show for the first time, that there are also concentrated regions of amorphous cellulose within the centre of anchor fibres (fibres that secure the pill head to the textile base; Fig. 1) and throughout the pill head (Fig. 5, Fig. 8, and Fig. 9). Whereas, the base (connection to main textile) of anchor fibres was predominately composed of more rigid crystalline cellulose (Fig. 8). This may explain why anchor fibres are often described as the more durable and stronger fibres compared to the pill head (Cooke, 1983; Long & Wei, 2004), as the increased regions of increased crystalline cellulose help secure the pill to the base of the textile.

Whilst no study has previously characterised and compared the localised distribution of amorphous and crystalline cellulose with such bioimaging techniques in cotton textile fibres, differences in the crystalline structure of different cellulosic fibres has been demonstrated. For example, Široký et al. (2012) highlight a semi-permeable skin and a porous core for lyocell fibres using crystalline (CBM2a, CBM3a, CBM10) and amorphous (CBM4-1, CBM17, CBM28) targeting CBMs, whereas previously, it was thought lyocell fibres comprise of an amorphous skin only (Bredereck & Hermanutz, 2005). For regular viscose rayon, Bredereck and Hermanutz (2005) describe the fibres have a 3:1 core-skin ratio, in which the core consists of a lower degree of crystalline regions compared to the skin. On the other hand, in bleached softwood kraft fibres there is a high degree of crystalline cellulose at the fibre surface interspersed by more amorphous regions (Novy et al., 2019). Therefore, it is likely cleaning (amorphous targeting) and care (crystalline targeting) cellulases will provide different pilling benefits for different regenerated cellulosic fibres compared to cotton textile fibres tested in this study, due to differences in crystallinity within the targeted substrate (Fig. 11).

Furthermore, in native cotton fibres the core consists of 40–60 % crystalline cellulose whilst the outer layer comprises of paracrystalline (mixture of crystalline and amorphous cellulose) depending on the species of *Gossypium* (Martínez-Sanz et al., 2017), which is similar to the findings here of cotton textile fibres. For textile applications, cotton fibres are spun into yarns for weaving or knitting into fabrics, and can be exposed to a variety of different harsh chemical processing steps, which include scouring, bleaching, mercerizing or dyeing (Runavot et al., 2014). For example, mercerization is used for some cotton fabrics to enhance tensile strength, water sorption, and improve dyeability and dimensional stability (Holme, 2016; Jordanov & Mangovska, 2009). However, this process irreversibly converts natural cotton of cellulose I

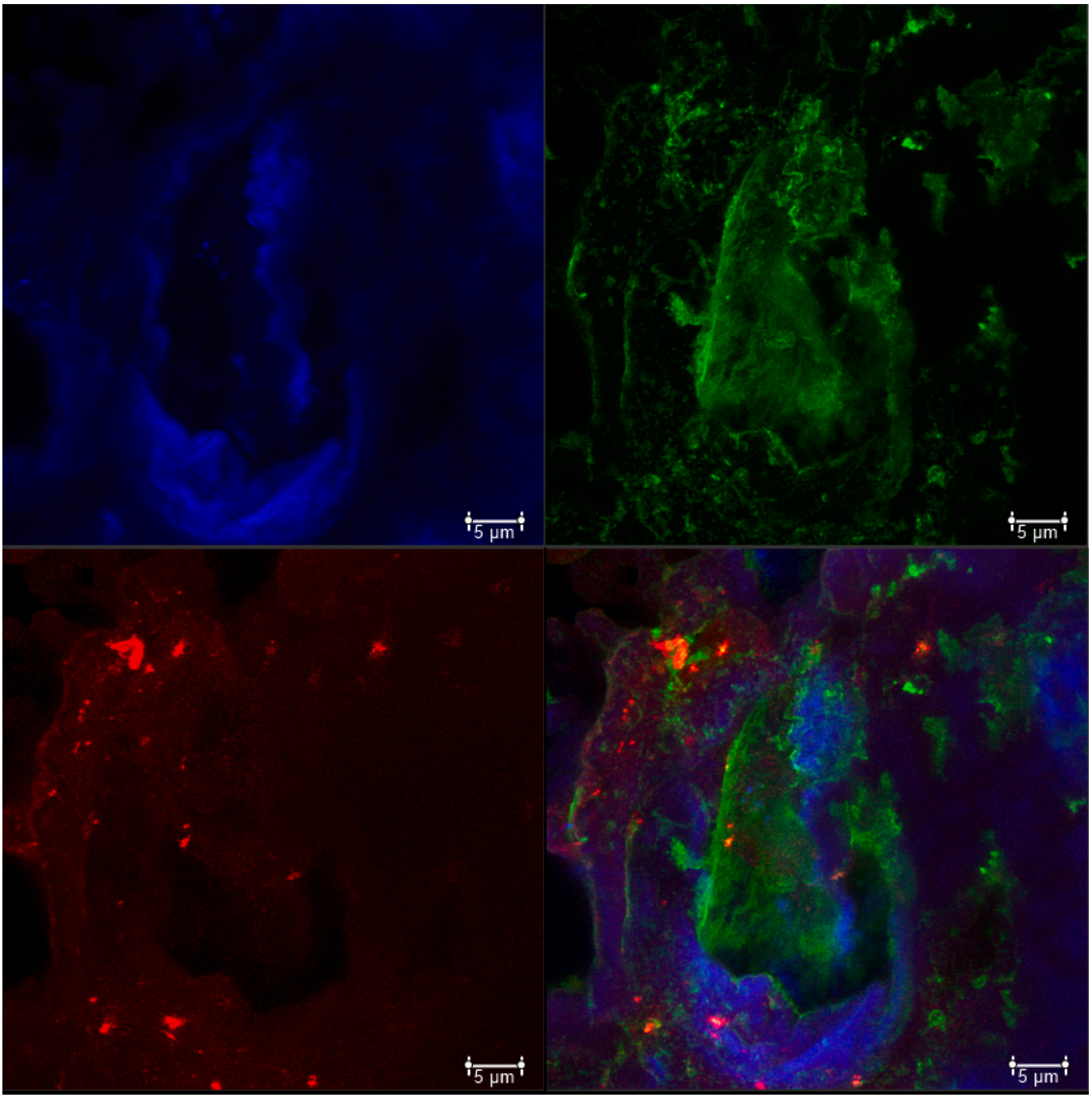

Fig. 7. Crystallinity cross section of anchor fibres. Crystalline (top right, green, using CBM2a-GFP) and amorphous (bottom left, red, CBM44-mCherry) cellulose distribution across the core cross section of a pilled anchor fibre, with the fibre outline (top left, blue, autofluorescence) and all channels overlaid (bottom right). Image acquired with a 60× oil lens and Leica SP8 confocal microscope.

into non-native cellulose II with a different crystal structure to natural cellulose (Okano & Sarko, 1985). Differences between cellulose I and II may be overlooked in the detergent industry when searching for novel pillase technologies as cellulases have evolved to degrade a subtly different material as cotton textile fibres are not native to the natural environment.

To aid in the search for new pillases, this study highlights the distribution of amorphous and crystalline cellulose can vary within a pill which is an important finding when elucidating how cellulases interact with pills as different enzymes will preferentially bind to different regions of the pill. Gourlay et al. (2015) used CBMs 2a and 44 with N-terminal fluorescent proteins to elucidate areas known as dislocations comprised of predominantly amorphous cellulose in dissolved hardwood pulp. These dislocations were described as weak points in the fibre from increased wear or damage, which can lead to fibre fragmentation. In this study, SEM and bioimaging techniques highlighted such dislocations are also found in the anchor fibre where the fibre is twisted and compressed (Fig. 2, Fig. 8, and Fig. 9). Pills on the surface of garments are more exposed to a high degree of abrasion that pull and twist the fibre (during wear or washing) altering the physical shape (which leads to the formation of pills, Fig. 1). Therefore, it is hypothesised that this physical process also leads to dislocations and subsequent concentrated regions of amorphous cellulose within the pill anchor fibre and pill head, where fibres may have fragmented (at dislocations) and become

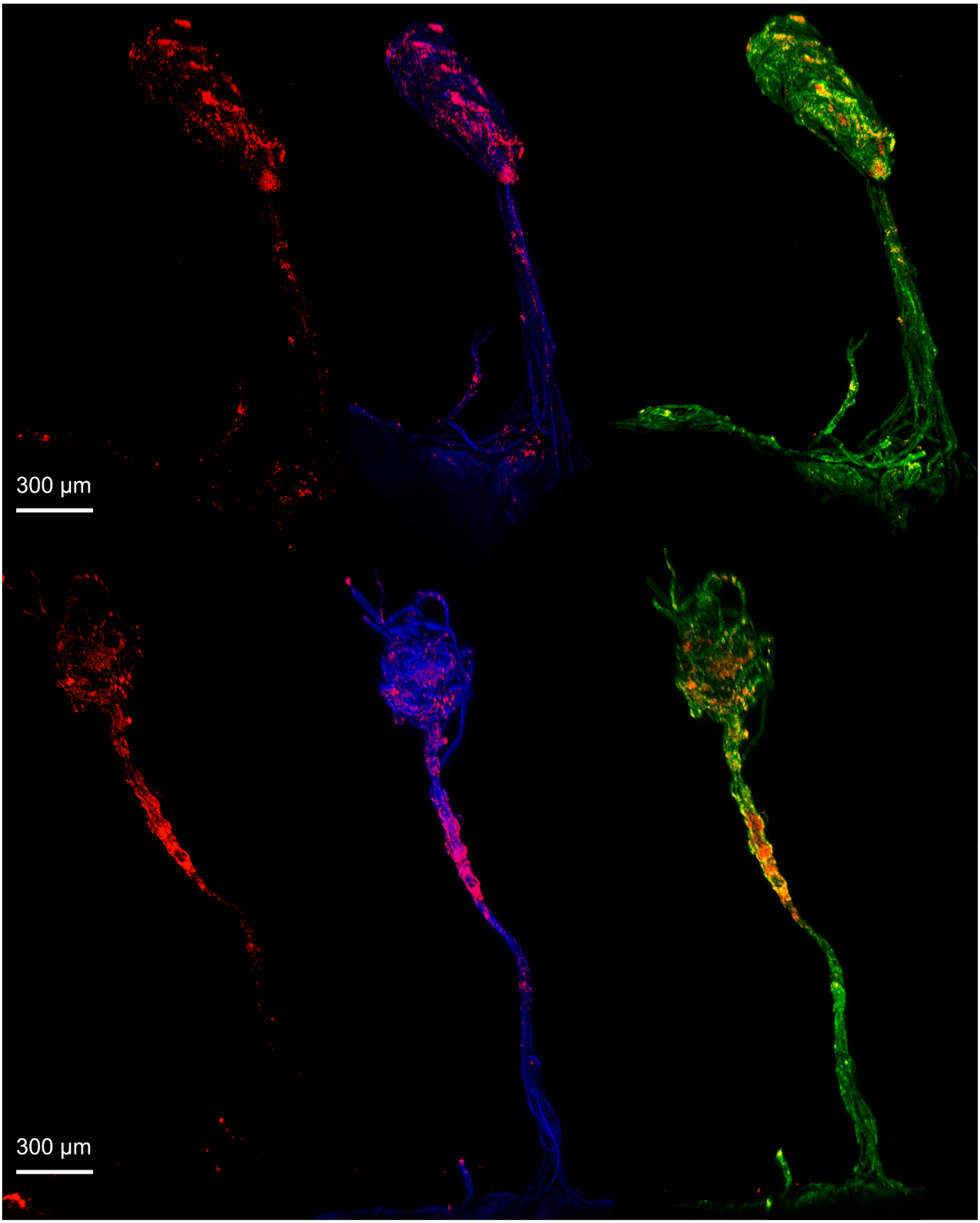

Fig. 8. Crystalline distribution within two different pills (top and bottom). Amorphous cellulose (red, using CBM44-mCherry) highlighted in all images, the pill outline highlighted by autofluorescence (blue) for contrast with amorphous cellulose (in the central two images) and all three fluorescence channels including crystalline cellulose (green, using CBM2a-GFP) to highlight concentrated regions of amorphous and crystalline cellulose (far right two images). Images acquired with Nikon A1R confocal microscope.

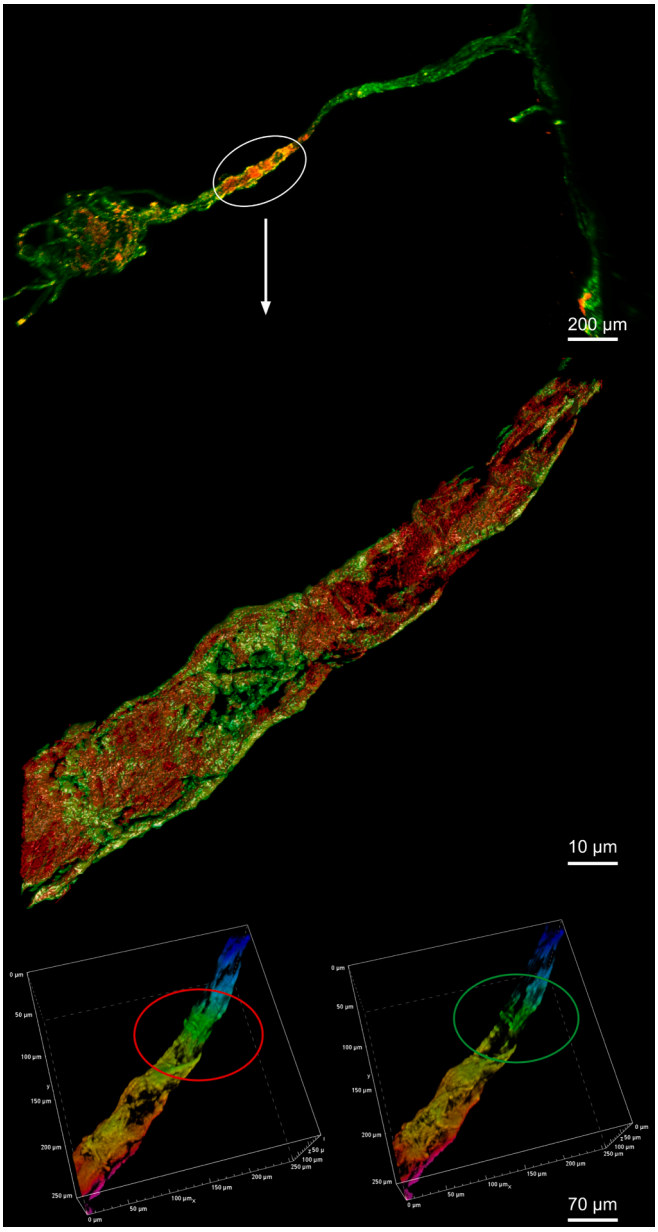

Fig. 9. Concentrated regions of amorphous cellulose in pills. Areas of amorphous (red, using CBM44-mCherry) and crystalline cellulose (green, using CBM2a-GFP) within a pill (top), highlighting a concentrated region of amorphous cellulose within the anchor fibre using a 3D render (middle) and a depth profile of the same region comparing the presence of amorphous cellulose (red circle, bottom left) and a lower concentration of crystalline cellulose (green circle, bottom right). Note within the depth profiles (bottom images), the colour of the fibre is irrespective of a fluorescence signal but highlights different depth positions along the focal plane. Images acquired with Nikon A1R confocal microscope.

incorporated into the entangled fibre matrix.

These regions of increased amorphous cellulose are more susceptible to enzymatic degradation (Hao et al., 2016; Pethrick, 2005) and may explain why some cleaning cellulases such as Biotouch® FLX1 and Whitezyme® can provide de-pilling benefits when targeting amorphous cellulose along the anchor fibre and pill head and highlights GH44 and GH45 families can provide greater pilling benefits than GH7 (Celluclean® 5000L) and GH5 (Celluclean® 5T) families (Fig. 11). However, Celluclean® 5000L is designed for improved whiteness benefits (as stated by the manufacturer, Novozymes), which may explain the apparent increase in pilling as DigiEye has detected the brighter (L*) white fibres protruding through the surface. Conversely, care cellulase can provide a greater de-pilling benefit (Fig. 11) as they are more likely to remove the pill all together from the anchor fibre base, which contains a higher degree of crystalline cellulose (Fig. 7). Therefore, this study provides visually evidence informing where different cellulases can preferentially target pills.

4.2. *Xyloglucan: a new target for 'pillase' discovery*

This study revealed the importance of xyloglucan in pilling for the first time, where pills contained 6.5 ± 3.6 times the concentration (fluorophore intensity) of xyloglucan compared to the main textile (Fig. 10). Xyloglucan comprise of a highly xylose-substituted β(1 –> 4) glucan backbone (Fry, 1989) and up to 75 % of the β-1,4- linked glucose residues are substituted with α-1-6-linked xylose side chains (Zhou et al., 2017). Xyloglucans are classified into two main types, the XXXG-type and XXGG-type based on regularity in the distribution of side chains (Vincken et al., 1997). XXXG-type consists of 3–4 glucose residues with a xylose side chain representing the main branching pattern of xyloglucan in plant cell walls. On the other hand, XXGG-type contains 2 or 4 consecutive glucose residues incorporating a xylose side chain representing the main branching pattern within plant seeds (Zhou et al., 2017). These xylose residues can also be found with a galactose residue sometimes attached to either fructose or arabinose residues (Obel et al., 2006). Hemicellulases, such as xyloglucans, amorphous cellulose, proteins and ions are found in the primary cell wall of plants that are hydrogen bonded to cellulose and enable the cross-linking of cellulose microfibrils providing a major load-baring structure, whereas the secondary wall contains only regions of crystalline cellulose (Kozłowski & Mackiewicz-Talarczyk, 2012; Rose, 2003; Zhou et al., 2007).

The primary cell wall of cotton fibres are also ensheathed in a waxy cuticle (Dochia et al., 2012). During textile processing, the cuticle and some non-cellulosic polysaccharide components can be removed (Jordanov & Mangovska, 2009). However, non-cellulosic polysaccharides are impacted differently depending on the textile treatment and hemicelluloses, such as xylan and xyloglucan, can be resistant to the harsh chemical processing (Runavot et al., 2014); yet, the potential role of these remaining hemicelluloses in pilling has not been thoroughly investigated. As SEM revealed a high degree of fraying along pilled fibres compared to the main textile fibres (Fig. 2 and Fig. 3), it was hypothesised that the reason for the increased concentration of xyloglucan in pills was due to surface abrasion of the fibres and fraying, exposing the underlying primary cell wall containing the hemicellulose components. This would therefore increase the opportunity for xyloglucan binding compared to the less frayed fibres within the main textile. In addition, the chain end action of *exo*-cellulases may be beneficial in attacking the frayed fibres of anchor strands rather than the internal action of *endo*-cellulase that have traditionally been the focus of detergent cellulases (Maurer & Gabler, 2016).

This study highlights targeting xyloglucan may provide a new and interesting opportunity to improve the benefit-to-risk paradigm as xyloglucanases are potentially more active towards pills than the main textile fibres, which would act to increase the pilling benefit (removal of pills), whilst reducing the potential tensile strength loss throughout the main textile.

Furthermore, Whitezyme® (GH44) preferentially cleaves cellulose but has also demonstrated some activity against substituted beta-1,4-glucan backbones in xyloglucan (Ariza et al., 2011) which may explain further, the pilling benefits observed with this enzyme compared to other cleaning enzymes that are not as active towards xyloglucan, such as Celluclean® 5T (Calvimontes et al., 2009) and Celluclean® 5000L (Jakob et al., 2020; Mackenzie et al., 1998) (Fig. 11). However, the use of a xyloglucan specific endo-beta-1,4 glucanase, which is not able to act on cellulose may provide a greater benefit by preferentially targeting pills and a reduced risk to tensile strength loss compared to

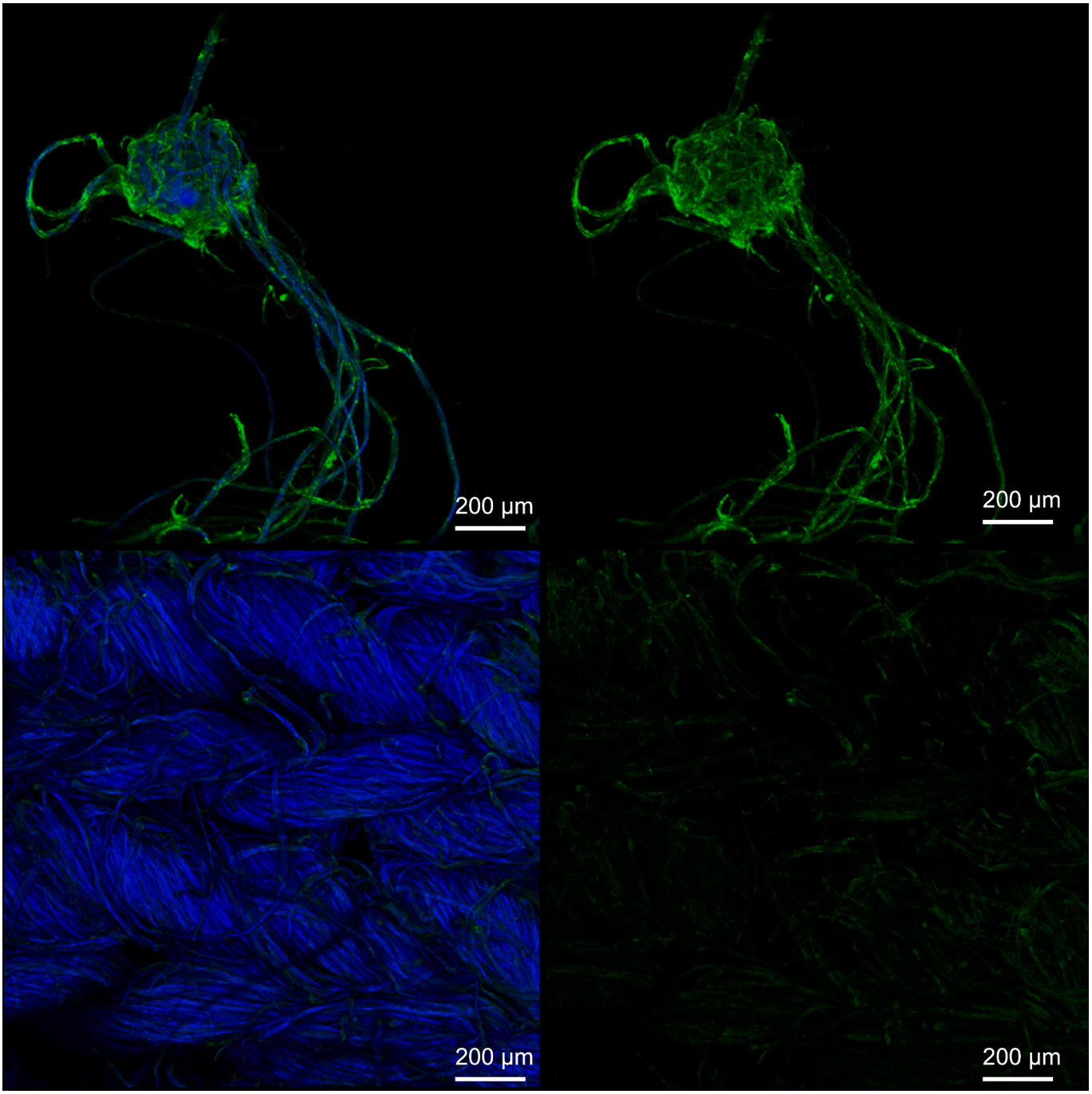

Fig. 10. Increased concentration of xyloglucan in a cotton textile pill compared to the main textile. The presence of xyloglucan (LM25-GFP) and the fibre outline (autofluorescence-blue) within a pill (top left); xyloglucan (LM25-GFP) within a pill only (average fluorophore intensity = 270, 388) (top right); xyloglucan and main textile fibres outlined (autofluorescence-blue) (bottom left); and xyloglucan (LM25-GFP) only within main textile fibres (average fluorophore intensity = 97, 020) (bottom right). Images acquired with Nikon A1R confocal microscope.

cellulase counterparts.

5. Conclusions

Using a suite of state-of-the-art bioimaging methods, this study confirms the hypothesis that there are localised differences in crystalline and amorphous cellulose throughout pills. Specifically, there are increased regions of amorphous cellulose within anchor fibres and throughout the pill head that are likely the result of fibre dislocations that form during increased wear and abrasion as fibres become twisted during pill development. Consequently, these regions of increased amorphous cellulose are weak points of the pill and may explain why some cleaning cellulases can also provide de-pilling benefits. On the other hand, the base of anchor fibres consisted of predominantly crystalline cellulose which is thought to enable the pill to maintain attachment to the textile and would need targeting by care cellulases for a superior pilling benefit to remove the pill entirely. This study also confirms the hypothesis that there are biophysical differences between pills and the main textile as we show there is 6.5× concentration of xyloglucan in cotton textile pills compared to fibres in the main textile. Therefore, xyloglucan provides a novel and specific target for providing pilling benefits where xyloglucanases and xyloglucan-debranching

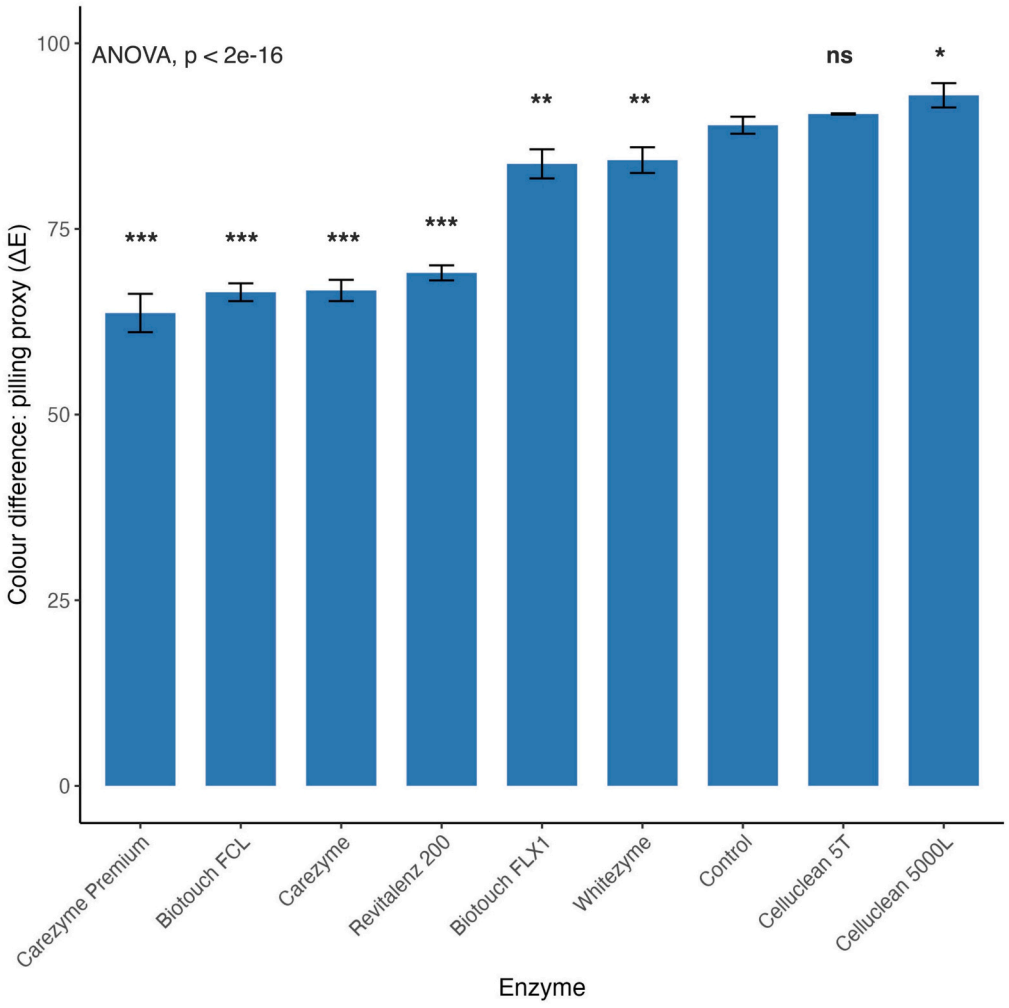

Fig. 11. Pilling performance of commercial enzymes (1 ppm) towards Swissatest® (252) fabric. A lower ΔE value, indicates greater pill removal. Significant differences indicated by Tukey's post-hoc analysis when compared to the control of Ariel® detergent only, highlighted by * ($P < 0.05$), ** ($P < 0.01$), or *** ($P < 0.001$).

enzymes offer a new avenue in the exploration of pillases for overcoming the benefit-to-risk paradigm.

CRediT authorship contribution statement

Max R. Kelly: Writing – original draft, Visualization, Methodology, Investigation, Formal analysis, Data curation, Conceptualization. **Neil J. Lant:** Writing – review & editing, Supervision, Resources, Investigation, Funding acquisition, Conceptualization. **Rolando Berlinguer-Palmini:** Writing – review & editing, Visualization, Software, Methodology, Investigation. **J. Grant Burgess:** Writing – review & editing, Supervision, Investigation, Funding acquisition, Conceptualization.

Declaration of competing interest

The authors declare the following financial interests/personal relationships which may be considered as potential competing interests: Neil Lant reports financial support was provided by Procter and Gamble. Neil Lant reports a relationship with Procter and Gamble that includes: employment. If there are other authors, they declare that they have no known competing financial interests or personal relationships that could have appeared to influence the work reported in this paper.

Data availability

Data will be made available on request.

Acknowledgements

We would like to thank the School of Chemistry (Newcastle University) and the technical staff for their services in X-ray diffraction for this study. We would also like to thank the Bioimaging unit at Newcastle University for their guidance and the Electron Microscopy Research Services team at Newcastle University for preparing samples for imaging.

Funding source

This work was funded by the Engineering and Physical Sciences Research Council (U.K.) and Procter and Gamble through an Industrial CASE studentship (EP/R512047/1).

Appendix A. Supplementary data

Supplementary data to this article can be found online at https://doi.org/10.1016/j.carbpol.2024.122243.

References

Aaron, J. S., Taylor, A. B., & Chew, T.-L. (2018). Image co-localization–co-occurrence versus correlation. *Journal of Cell Science, 131*(3), Article jcs211847.

Alapuranen, M., Valtakari, L., Kallio, J., Ojapalo, P., & Vehmaanperä, J. (2007). Enzyme fusion proteins and their use. In *Google patents*.

Al-Ghanayem, A. A., & Joseph, B. (2020). Current prospective in using cold-active enzymes as eco-friendly detergent additive. *Applied Microbiology and Biotechnology, 104*(7), 2871–2882.

Ansell, M. P., & Mwaikambo, L. Y. (2009). The structure of cotton and other plant fibres. In *Handbook of textile fibre structure* (pp. 62–94). Elsevier.

Ariza, A., Eklöf, J. M., Spadiut, O., Offen, W. A., Roberts, S. M., Besenmatter, W., … Brumer, H. (2011). Structure and activity of *Paenibacillus polymyxa* xyloglucanase from glycoside hydrolase family 44. *Journal of Biological Chemistry, 286*(39), 33890–33900.

Arja, M.-O. (2007). Cellulases in the textile industry. In *Industrial enzymes* (pp. 51–63). Springer.

Baird, M., Hatfield, P., & Morris, G. (1956). 12-Pilling of fabrics: A study of nylon and nylon blended fabrics. *Journal of the Textile Institute Transactions, 47*(4), T181–T201.

Biggs, D. S. C. (2010). 3D deconvolution microscopy. *Current Protocols in Cytometry, 52* (1), Article 12.19.11-12.19.20. https://doi.org/10.1002/0471142956.cy1219s52

Boraston, A. B., Bolam, D. N., Gilbert, H. J., & Davies, G. J. (2004). Carbohydrate-binding modules: Fine-tuning polysaccharide recognition. *Biochemical Journal, 382*(3), 769–781.

Boraston, A. B., Revett, T. J., Boraston, C. M., Nurizzo, D., & Davies, G. J. (2003). Structural and thermodynamic dissection of specific mannan recognition by a carbohydrate binding module, TmCBM27. *Structure, 11*(6), 665–675.

Bredereck, K., & Hermanutz, F. (2005). Man–made cellulosics. *Review of Progress in Coloration and Related Topics, 35*(1), 59–75.

Bui, H. M., Ehrhardt, A., & Bechtold, T. (2008). Pilling in cellulosic fabrics, part 2: A study on kinetics of pilling in alkali-treated lyocell fabrics. *Journal of Applied Polymer Science, 109*(6), 3696–3703.

Calvimontes, A., Stamm, M., & Dutschk, V. (2009). Effect of cellulase enzyme on cellulose nano-topography. *Tenside Surfactants Detergents, 46*(6), 368–372.

Caparrós, C., Lant, N., Smets, J., & Cavaco-Paulo, A. (2012). Effects of adsorption properties and mechanical agitation of two detergent cellulases towards cotton cellulose. *Biocatalysis and Biotransformation, 30*(2), 260–271.

Choudhury, A. K. R. (2017). *Principles of textile finishing*. Woodhead Publishing.

Cooke, W. (1983). 10 - The influence of fibre fatigue on the pilling cycle part II: Fibre entanglement and pill growth. *Journal of the Textile Institute, 74*(3), 101–108.

Cooper, T., Claxton, S., Hill, H., Holbrook, K., Hughes, M., Knox, A., & Oxborrow, L. (2013). Development of an industry protocol on clothing longevity. In *Report produced for Waste and Resources Action Programme (WRAP)*. Nottingham: Trent University Nottingham.

Davies, G. J., Dodson, G., Moore, M. H., Tolley, S. P., Dauter, Z., Wilson, K. S., … Schülein, M. (1996). Structure determination and refinement of the *Humicola insolens* endoglucanase V at 1.5 Å resolution. *Acta Crystallographica Section D: Biological Crystallography, 52*(1), 7–17.

Derhak, M. W. (2015). *Spectrally based material color equivalency: Modeling and manipulation*. Rochester Institute of Technology.

Dochia, M., Sirghie, C., Kozłowski, R., & Roskwitalski, Z. (2012). Cotton fibres. In *Handbook of natural fibres* (pp. 11–23). Elsevier.

EMF. (2017). A new textiles economy: Redesigning fashions future. Retrieved 3 June 2019, from https://www.ellenmacarthurfoundation.org/assets/downloads/publications/A-New-Textiles-Economy_Full-Report_Updated_1-12-17.pdf.

Fry, S. C. (1989). The structure and functions of xyloglucan. *Journal of Experimental Botany, 40*(1), 1–11.

Ghaffar, S. (2017). Straw fibre-based construction materials. In *Advanced high strength natural fibre composites in construction* (pp. 257–283). Elsevier.

Gintis, D., & Mead, E. J. (1959). The mechanism of pilling. *Textile Research Journal, 29* (7), 578–585.

Gourlay, K., Hu, J., Arantes, V., Penttilä, M., & Saddler, J. N. (2015). The use of carbohydrate binding modules (CBMs) to monitor changes in fragmentation and cellulose fiber surface morphology during cellulase-and swollenin-induced deconstruction of lignocellulosic substrates. *Journal of Biological Chemistry, 290*(5), 2938–2945.

Hansen, C. D., & Johnson, C. R. (2011). *Visualization handbook*. Elsevier.

Hao, L., Wang, R., Wang, L., Fang, K., Liu, J., & Men, Y. (2016). The influences of enzymatic processing on physico-chemical and pigment dyeing characteristics of cotton fabrics. *Cellulose, 23*(1), 929–940.

Hewetson, B. B., Zhang, X., & Mosier, N. S. (2016). Enhanced acid-catalyzed biomass conversion to hydroxymethylfurfural following cellulose solvent-and organic solvent-based lignocellulosic fractionation pretreatment. *Energy & Fuels, 30*(11), 9975–9977.

Holme, I. (2016). Coloration of technical textiles. In *Handbook of technical textiles* (pp. 231–284). Elsevier.

Jakob, C., O'connell, T., Jochens, H., Wallrapp, F., Hoesl, M., Kohl, A., … Kotsakis, P. (2020). Cellulase suitable for use in detergent compositions. In *Google patents*.

Jauris, S., Rücknagel, K. P., Schwarz, W. H., Kratzsch, P., Bronnenmeier, K., & Staudenbauer, W. L. (1990). Sequence analysis of the Clostridium stercorarium celZ gene encoding a thermoactive cellulase (Avicelase I): Identification of catalytic and cellulose-binding domains. *Molecular and General Genetics MGG, 223*(2), 258–267.

Jordanov, I., & Mangovska, B. (2009). Characterization on surface of mercerized and enzymatic scoured cotton after different temperature of drying. *The Open Textile Journal, 2*(1).

Juntunen, K., Alapuranen, M., Valtakari, L., Meriläinen, H.-M., & Puranen, T. (2018). Fungal endoglucanase variants, their production and use. In *Google patents*.

Juntunen, K., Valtakari, L., Mäkinen, S., Alapuranen, M., Hellmuth, H., Ojapalo, P., Mennicken, M., Schwaneberg, U., Schönauer, D., & Puranen, T. (2020). Variants of fungal cellulase. In *Google patents*.

Koga, J., Baba, Y., Shimonaka, A., Nishimura, T., Hanamura, S., & Kono, T. (2008). Purification and characterization of a new family 45 endoglucanase, STCE1, from *Staphylotrichum coccosporum* and its overproduction in *Humicola insolens*. *Applied and Environmental Microbiology, 74*(13), 4210–4217.

Kozłowski, R., & Mackiewicz-Talarczyk, M. (2012). *Handbook of natural fibres*. Elsevier.

Krichevsky, O., & Bonnet, G. (2002). Fluorescence correlation spectroscopy: The technique and its applications. *Reports on Progress in Physics, 65*(2), 251.

Landau, H. (1967). Sampling, data transmission, and the Nyquist rate. *Proceedings of the IEEE, 55*(10), 1701–1706.

Long, L., & Wei, Z. (2004). Pilling of polyester/wool blends. *Indian Journal of Fibre and Textile Research, 29*, 480–482.

Luo, M., Cui, C., & Li, C. (2001). *British patent (Application No. 0124683.4) entitled apparatus and method for measuring colour (DigiEye® System). Derby University Enterprises Limited*.

Mackenzie, L. F., Sulzenbacher, G., Divine, C., Jones, T. A., Wöldike, H. F., Schülein, M., … Davies, G. J. (1998). Crystal structure of the family 7 endoglucanase I (Cel7B) from *Humicola insolens* at 2.2 Å resolution and identification of the catalytic nucleophile by trapping of the covalent glycosyl-enzyme intermediate. *Biochemical Journal, 335*(2), 409–416.

Marcus, S. E., Blake, A. W., Benians, T. A., Lee, K. J., Poyser, C., Donaldson, L., … Boraston, A. (2010). Restricted access of proteins to mannan polysaccharides in intact plant cell walls. *The Plant Journal, 64*(2), 191–203.

Marcus, S. E., Verhertbruggen, Y., Hervé, C., Ordaz-Ortiz, J. J., Farkas, V., Pedersen, H. L., … Knox, J. P. (2008). Pectic homogalacturonan masks abundant sets of xyloglucan epitopes in plant cell walls. *BMC Plant Biology, 8*(1), 1–12.

Martínez-Sanz, M., Pettolino, F., Flanagan, B., Gidley, M. J., & Gilbert, E. P. (2017). Structure of cellulose microfibrils in mature cotton fibres. *Carbohydrate Polymers, 175*, 450–463.

Maurer, K. H. (1997). Development of new cellulases. *Surfactant Science Series*, 175–202.

Maurer, K.-H., & Gabler, M. (2016). Analysis of detergent enzymes. In *Handbook Of Detergents, Part C* (pp. 489–504). CRC Press.

Montazer, M., & Sadighi, A. (2006). Optimization of the hot alkali treatment of polyester/cotton fabric with sodium hydrosulfite. *Journal of Applied Polymer Science, 100*(6), 5049–5055.

Moraïs, S., Stern, J., Kahn, A., Galanopoulou, A. P., Yoav, S., Shamshoum, M., … Bayer, E. A. (2016). Enhancement of cellulosome-mediated deconstruction of cellulose by improving enzyme thermostability. *Biotechnology for Biofuels, 9*(1), 1–12.

Morgado, J., Cavaco-Paulo, A., & Rousselle, M.-A. (2000). Enzymatic treatment of lyocell—Clarification of depilling mechanisms. *Textile Research Journal, 70*(8), 696–699.

Niyonzima, F. N. (2019). Detergent-compatible bacterial cellulases. *Journal of Basic Microbiology, 59*(2), 134–147.

Novy, V., Aïssa, K., Nielsen, F., Straus, S. K., Ciesielski, P., Hunt, C. G., & Saddler, J. (2019). Quantifying cellulose accessibility during enzyme-mediated deconstruction using 2 fluorescence-tagged carbohydrate-binding modules. *Proceedings of the National Academy of Sciences, 116*(45), 22545–22551.

Obel, N., Neumetzler, L., & Pauly, M. (2006). Hemicelluloses and cell expansion. In *The expanding cell* (pp. 57–88). Springer.

Okano, T., & Sarko, A. (1985). Mercerization of cellulose. II. Alkali–cellulose intermediates and a possible mercerization mechanism. *Journal of Applied Polymer Science, 30*(1), 325–332.

Pedersen, H. L., Fangel, J. U., McCleary, B., Ruzanski, C., Rydahl, M. G., Ralet, M.-C., … Andersen, M. C. (2012). Versatile high resolution oligosaccharide microarrays for plant glycobiology and cell wall research. *Journal of Biological Chemistry, 287*(47), 39429–39438.

Pethrick, R. A. (2005). Polymer structures. In F. Bassani, G. L. Liedl, & P. Wyder (Eds.), *Encyclopedia of condensed matter physics* (pp. 355–362). Elsevier.

Raghothama, S., Simpson, P. J., Szabó, L., Nagy, T., Gilbert, H. J., & Williamson, M. P. (2000). Solution structure of the CBM10 cellulose binding module from *Pseudomonas* xylanase A. *Biochemistry, 39*(5), 978–984.

Robertson, A. R. (1977). The CIE 1976 color-difference formulae. *Color Research & Application, 2*(1), 7–11.

Rose, J. K. (2003). *The plant cell wall* (vol. 8). Blackwell Publishing.

Rous, M. A., Ingolic, E., & Schuster, K. C. (2006). Visualisation of the fibrillar and pore morphology of cellulosic fibres applying transmission electron microscopy. *Cellulose, 13*(4), 411–419.

Runavot, J. L., Guo, X., Willats, W. G., Knox, J. P., Goubet, F., & Meulewaeter, F. (2014). Non-cellulosic polysaccharides from cotton fibre are differently impacted by textile processing. *PLoS One, 9*(12), Article e115150.

Schou, C., Rasmussen, G., Kaltoft, M. B., Henrissat, B., & Schülein, M. (1993). Stereochemistry, specificity and kinetics of the hydrolysis of reduced cellodextrins by nine cellulases. *European Journal of Biochemistry, 217*(3), 947–953.

Schülein, M. (2000). Protein engineering of cellulases. *Biochimica et Biophysica Acta (BBA)-Protein Structure and Molecular Enzymology, 1543*(2), 239–252.

Segal, L., Creely, J., Martin, A., Jr., & Conrad, C. (1959). An empirical method for estimating the degree of crystallinity of native cellulose using the X-ray diffractometer. *Textile Research Journal, 29*(10), 786–794.

Simpson, P. J., Xie, H., Bolam, D. N., Gilbert, H. J., & Williamson, M. P. (2000). The structural basis for the ligand specificity of family 2 carbohydrate-binding modules. *Journal of Biological Chemistry, 275*(52), 41137–41142.

Singh, S., Tank, N. K., Dwiwedi, P., Charan, J., Kaur, R., Sidhu, P., & Chugh, V. K. (2018). Monoclonal antibodies: A review. *Current Clinical Pharmacology, 13*(2), 85–99.
Široký, J., Benians, T. A., Russell, S. J., Bechtold, T., Knox, J. P., & Blackburn, R. S. (2012). Analysis of crystallinity changes in cellulose II polymers using carbohydrate-binding modules. *Carbohydrate Polymers, 89*(1), 213–221.
Stryckman, J., & Leclereq, F. (1972). *Methods and finishes for reducing pilling. Part I. Wool science review. 42* pp. 32–45).
Tkalcic, M., & Tasic, J. F. (2003). Colour spaces: Perceptual, historical and applicational background. In *, vol. 1. IEEE region 8 Eurocon conference, computer as a tool*.
Tomasino, C. (1992). *Chemistry and technology of fabric preparation and finishing*. Chemistry and Science College of Textiles: Department of Textile Engineering.
Ukponmwan, J., Mukhopadhyay, A., & Chatterjee, K. (1998). Pilling. *Textile Progress, 28*(3), 1–57.
van Bueren, A. L., Morland, C., Gilbert, H. J., & Boraston, A. B. (2005). Family 6 carbohydrate binding modules recognize the non-reducing end of β-1, 3-linked glucans by presenting a unique ligand binding surface. *Journal of Biological Chemistry, 280*(1), 530–537.
Vincken, J.-P., York, W. S., Beldman, G., & Voragen, A. (1997). Two general branching patterns of xyloglucan, XXXG and XXGG. *Plant Physiology, 114*(1), 9.
Willats, W. G., Orfila, C., Limberg, G., Buchholt, H. C., van Alebeek, G.-J. W., Voragen, A. G., … Murray, B. S. (2001). Modulation of the degree and pattern of methyl-esterification of pectic homogalacturonan in plant cell walls: Implications for pectin methyl esterase action, matrix properties, and cell adhesion. *Journal of Biological Chemistry, 276*(22), 19404–19413.
Zhou, Q., Rutland, M. W., Teeri, T. T., & Brumer, H. (2007). Xyloglucan in cellulose modification. *Cellulose, 14*(6), 625–641.
Zhou, X., Li, W., Mabon, R., & Broadbelt, L. J. (2017). A critical review on hemicellulose pyrolysis. *Energy Technology, 5*(1), 52–79.